Ultrafast Science
A SCIENCE PARTNER JOURNAL

RESEARCH ARTICLE

Rapid-Scan Nonlinear Time-Resolved Spectroscopy over Arbitrary Delay Intervals

Tobias Flöry[1*], Vinzenz Stummer[1], Justinas Pupeikis[2], Benjamin Willenberg[2], Alexander Nussbaum-Lapping[2], Edgar Kaksis[1], Franco V. A. Camargo[3], Martynas Barkauskas[4], Christopher R. Phillips[2], Ursula Keller[2], Giulio Cerullo[3,5], Audrius Pugžlys[1,6], and Andrius Baltuška[1,6]

[1]Photonics Institute, TU Wien, Vienna, Austria. [2]Department of Physics, ETH Zurich, Zurich, Switzerland. [3]Istituto di Fotonica e Nanotecnologie-CNR, Piazza Leonardo da Vinci 32, 20133 Milano, Italy. [4]Light Conversion Ltd., Vilnius, Lithuania. [5]Dipartimento di Fisica, Politecnico di Milano, Piazza Leonardo da Vinci 32, 20133 Milano, Italy. [6]Center for Physical Sciences & Technology, Savanoriu Ave. 231 LT-02300, Vilnius, Lithuania.

*Address correspondence to: tobias.floery@tuwien.ac.at

Citation: Flöry T, Stummer V, Pupeikis J, Willenberg B, Nussbaum-Lapping A, Kaksis E, Camargo FVA, Barkauskas M, Phillips CR, Keller U, et al. Rapid-Scan Nonlinear Time-Resolved Spectroscopy over Arbitrary Delay Intervals. *Ultrafast Sci.* 2023;3:Article 0027. https://doi.org/10.34133/ultrafastscience.0027

Submitted 14 December 2022
Accepted 29 March 2023
Published 18 May 2023

Femtosecond dual-comb lasers have revolutionized linear Fourier-domain spectroscopy by offering a rapid motion-free, precise, and accurate measurement mode with easy registration of the combs beat note in the radio frequency domain. Extensions of this technique already found application for nonlinear time-resolved spectroscopy within the energy limit available from sources operating at the full oscillator repetition rate. Here, we present a technique based on time filtering of femtosecond frequency combs by pulse gating in a laser amplifier. This gives the required boost to the pulse energy and provides the flexibility to engineer pairs of arbitrarily delayed wavelength-tunable pulses for pump–probe techniques. Using a dual-channel millijoule amplifier, we demonstrate programmable generation of both extremely short, fs, and extremely long (>ns) interpulse delays. A predetermined arbitrarily chosen interpulse delay can be directly realized in each successive amplifier shot, eliminating the massive waiting time required to alter the delay setting by means of an optomechanical line or an asynchronous scan of 2 free-running oscillators. We confirm the versatility of this delay generation method by measuring $\chi^{(2)}$ cross-correlation and $\chi^{(3)}$ multicomponent population recovery kinetics.

Introduction

Ultrafast pump–probe spectroscopy is a very powerful technique to investigate the dynamics of photoinduced processes in a variety of systems, from (bio)-molecules to solids. It is typically performed in a stroboscopic fashion, whereby, at first, a pump pulse excites the system and its photoinduced absorption/reflection change is monitored by a time-delayed probe pulse. Typically, the pump and probe pulses are derived from the same laser source, often using nonlinear optical frequency conversion to obtain photon energies matching the energy levels of the samples and a mechanical delay line to control their timing up to a delay of a few nanoseconds [1]. However, many processes, such as ligand rebinding in proteins [2] and charge recombination in photovoltaic devices [3], occur over a multitude of time scales, from fs to μs, which cannot be accessed by mechanical delays. In addition, delay lines require careful alignment to avoid lateral beam drifts and may suffer from spurious signal variations due to a change of the focused beam diameter induced by divergence. For these reasons, sources of synchronized, high-energy pulses whose delay can be electronically controlled over a wide range without moving optical arms would be advantageous.

Femtosecond dual-comb sources operating at MHz to GHz repetition rate have revolutionized frequency metrology and linear Fourier-domain spectroscopy by offering an interpulse delay scanning mode, known as equivalent time sampling and in specific configurations ASynchronous Optical Sampling (ASOPS) [4,5], both without the need for a mechanically steered optical delay line and its associated shortcomings for large (>ns) interpulse delays [6,7].

While a powerful technique, ASOPS is not suitable for generating a sufficient dynamic range for time-resolved spectroscopy on a broad class of higher-order nonlinear susceptibilities. Firstly, the interpulse delay increment is fixed, which does not allow for efficient sampling of complex dynamics extending over multiple time scales. Furthermore, the pulse energy is limited since amplifying a laser oscillator at its full repetition rate implies a high average power (with corresponding technical challenges on the laser source and thermal damage on the sample). The short inter-pulse spacing also limits the scan range, and the measurements are susceptible to the accumulation of long-lived components, e.g., population of triplet states [8]; such artifacts are a typical challenge of third- and higher-order nonlinear spectroscopies. Importantly for our further discussion, even if the single-pulse energy at a full

oscillator repetition rate is boosted to a level sufficient for parametric frequency conversion and/or for pump–probe signal generation, there will remain numerous problems with the acquisition of kinetics. One prominent problem is the inability to average the nonlinear signal at a fixed delay point and a substantial waiting time before the same delay point can be revisited again. The waiting time grows inversely proportional to the time-resolution step determined by the detuning of the 2 cavities.

Dividing up the MHz repetition rate of a master oscillator by capturing a selected pulse in a kHz multipass or regenerative amplifier (RA) allows for the generation of fully electronically tunable interpulse delays, as shown in several published schemes [9–11]. The most intuitive approach is to seed 2 RA cavities from a common oscillator; by either selecting different oscillator pulses or by using different lengths of the amplification window, pulse spacings in the order of the oscillator repetition period can be generated [12]. This method allows the generation of arbitrarily long interpulse delays at the expense of nanosecond resolution. Fully electronically tunable delays over a broad range were demonstrated by Bredenbeck et al. [9], using 2 electronically synchronized mode-locked oscillators seeding 2 individually controlled RAs. However, the time resolution was limited to 1.8 ps due to synchronization jitter between the oscillators.

Another interesting development is the (kHz-) Arbitrary Detuning–ASOPS (AD-ASOPS) technique [13–15]. Instead of relying on 2 synchronized oscillators, 2 deliberately strongly detuned oscillators with a correspondingly short beat period are used to seed 2 RAs. The instantaneous frequency of the 2 oscillators together with a coincidence event are continuously monitored and evaluated. Notably, it is also possible to recover shorter time delays on a sub-ps scale by post-calibrating the measured results, for example, by evaluating the spectral interference fringes of the amplified pulses. The inconvenience, ultimately translated into substantially longer acquisition times, is that the appearance of a particular delay setting within an expected delay range becomes statistical [9–11].

Materials and Methods

Here, we report a method capable of a deterministic control of time delay scans from fs to ms with femtosecond accuracy, which overcomes most problems arising in both opto-mechanical delay generation and in earlier attempts at electronic delay control and recovery. Our method is enabled by the use of a low-noise, spatially multiplexed, single-cavity, femtosecond, dual-comb oscillator similar to the one presented in [16]. While this can also be accomplished by 2 synchronized oscillators [17,18], the intrinsic lower noise and experimental setup simplicity of the single-cavity dual-comb enabled us to achieve sub-100-fs jitter at arbitrary delays between the amplified pulses.

Figure 1 shows the conceptual scheme of the system. A dual-comb oscillator (Yb:CaF_2, $\lambda = 1{,}050$ nm) delivers 2 femtosecond pulse trains with 2.0 W average power each at a repetition rate $f_{rep1,2} \cong 80$ MHz and a repetition-rate detuning of $\Delta f_{rep} \cong 500$ Hz. This results in a time delay increment between consecutive pulses $\Delta t = 1/f_{rep1} - 1/f_{rep2} \approx \Delta f_{rep}/(f_{rep1,2})^2 \approx 80$ fs. A fraction of the oscillator output is directed toward a cross-correlation setup used to detect the temporal overlap of the pulse trains by generating the sum-frequency signal in a β-barium borate (BBO) nonlinear crystal in type I phase matching configuration.

This signal is detected (PDA10A2, 150 MHz bandwidth) to obtain a trigger "start" signal for the timing electronics. The pulses are stretched in a common grating-based stretcher and amplified in 2 RA cavities (Yb:CaF_2, ~600 fs pulse duration, 1 mJ pulse energies; further details in the Supplementary Materials) built as a monolithic block pumped by a single laser diode. The amplified pulses are then recompressed in a compressor employing a single transmission diffraction grating but 2 separated beam paths. The RAs employ Pockels cells in order to select single oscillator pulses and control the amplification window. A fresh amplification cycle is started with a certain waiting period to select a pulse pair with the desired delay, every time a pulse overlap is detected by the cross-correlation setup. Therefore, the RAs operate at a repetition rate corresponding to the oscillator detuning frequency $f_{RA} = \Delta f_{rep} = 500$ Hz.

Figure 2 shows a typical time trace of the pulse train emitted by the dual-comb oscillator. Due to the detuning of the oscillator repetition rates, the pulse delay increases from one pulse pair to the next with a defined increment Δt. Thereupon, by selecting the pulses of the oscillator pulse trains OSC1 and OSC2, with pulse indices n and m, respectively, a pulse pair with a defined time delay $\tau = m/f_{rep2} - n/f_{rep1}$ can be selected. For equal pulse indices ($n = m$), this leads to a time delay of $\tau = n\,(1/f_{rep2} - 1/f_{rep1}) \cong n\,\Delta t$. This allows for the generation of

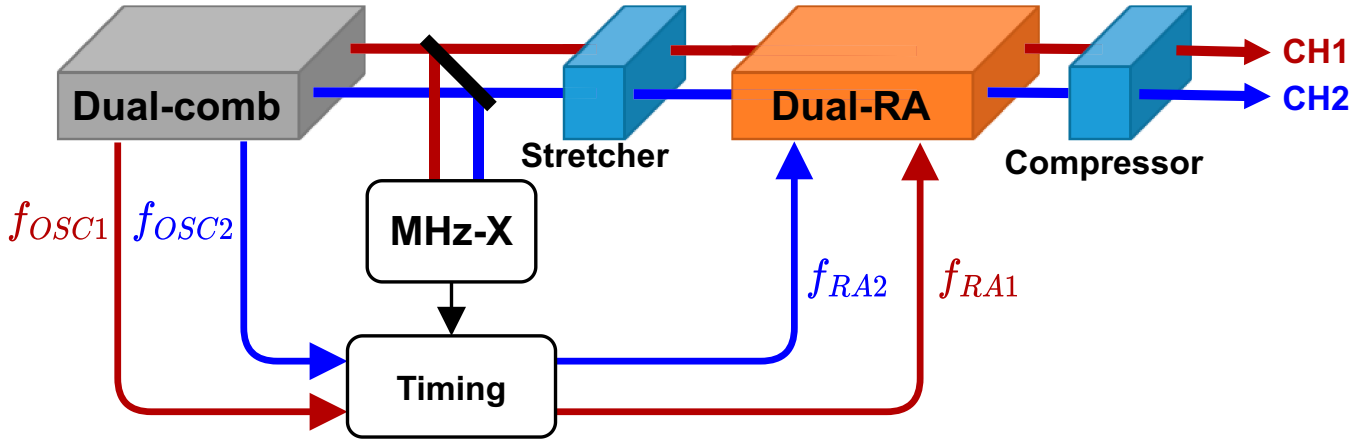

Fig. 1. System setup. MHz-X: cross-correlation of the 2 pulse trains at the full repetition rate for zero overlap detection. Timing: Timing electronics for the RAs.

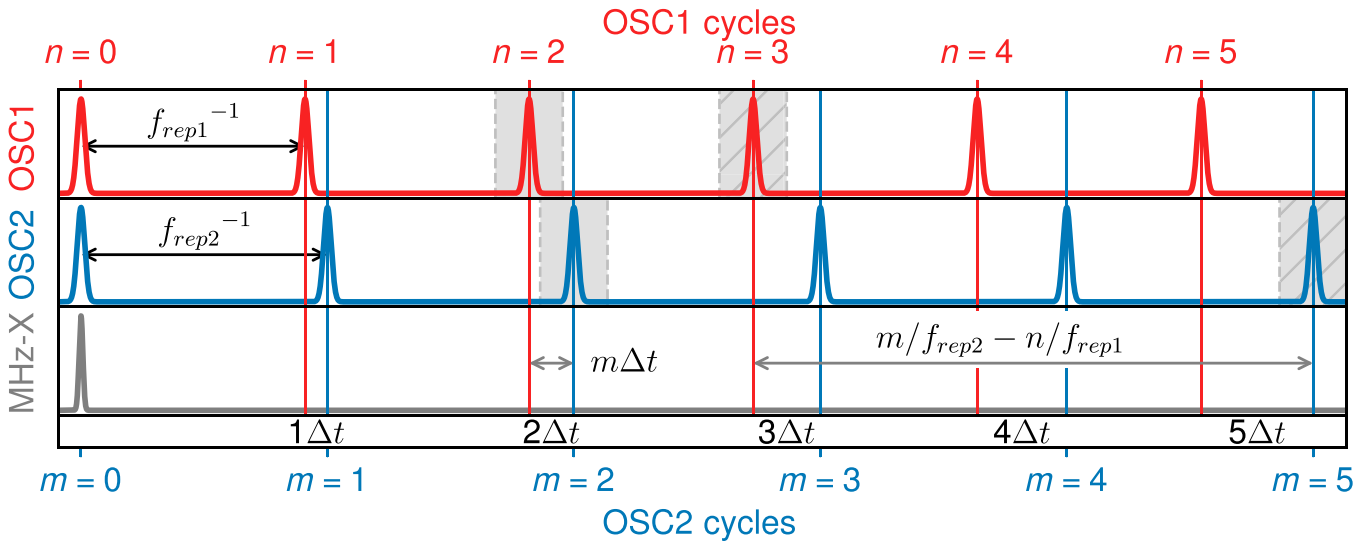

Fig. 2. Operating principle: the top trace shows pulses from OSC1; the middle trace shows the pulses from OSC2; bottom: cross-correlation between OSC1 and OSC2. Shaded areas indicate pulses selected for amplification for 2 cases: gray: $\Delta t < 1/f_{rep1,2}$, hatched gray: $\Delta t > 1/f_{rep1,2}$.

time delays with a step size down to $\Delta t = \Delta f_{rep}/(f_{rep1,2})^2 \approx 80$ fs within a time window from zero optical delay to the inverse oscillator repetition rate $1/f_{rep1,2} \cong 12.5$ ns. The latter limitation can be overcome by choosing different waiting times (i.e., pulse indices) for the 2 channels, e.g., $m = n + k$, so that $\tau = n\,\Delta t + k/f_{rep2}$. The pulse indices (m,n) and the corresponding interpulse delay are selected by counting the pulses in the respective channel starting from the cross-correlation event and then switching the Pockels cells to start the amplification window. The counting of the pulses from the start event can be performed by either home-built electronic counters or off-the-shelf delay generators. In our particular case, the BME_SG08p (Bergmann Messgeräte Entwicklung KG) was used. Therefore, the interpulse delay can be set on a shot-to-shot basis over the whole range. Furthermore, it is possible to remain at a certain time delay for an arbitrary amount of time by not adjusting the amplification window, allowing one to accumulate and average the corresponding transient absorption signal to improve the signal-to-noise ratio. For interpulse delays in the range of the inverse oscillator roundtrip time, the system can also be operated in an ASOPS manner by ignoring the cross-correlation signal and firing the RAs at a fixed repetition rate (f_{RA}). Details for this mode can be found in the Supplementary Materials.

Single-cavity dual-comb lasers can provide few-femtosecond relative timing jitter [16]. However, at long time scales, the relative timing is subject to drifts due to thermal variation in the environment. In our case, we have used a single-cavity dual-comb laser for which the repetition rate difference Δf_{rep} was stabilized [16]. This stabilization could be avoided by live tracking of the repetition rate difference and recalculating the time delay on a shot-to-shot basis. Using equation 12 from [19], one can estimate the period jitter for the used oscillator to be in the order of 4 fs, which is the determining uncertainty for any pulse pair selected within a 2-ms ($=1/f_{RA} = 1/\Delta f_{rep}$) time window.

Results and Discussion

As a proof-of-principle demonstration, a cross-correlation measurement of the amplified output pulses was performed. For this measurement, the amplified pulses were focused and overlapped, using a single lens, into a BBO crystal and the sum-frequency output signal was recorded using a biased photodiode (Thorlabs DET10A, 350 MHz bandwidth). To suppress scattered light from the fundamental beams, an aperture and optical short-pass filters were installed before the photodiode.

Figure 3 shows the result of the cross-correlation measurements with ~80 fs step size. Figure 3A shows the direct result, while for Fig. 3B, the pulse compressor parameters for one of the channels were changed, by adjusting the optical path length, resulting in a longer output pulse in the corresponding channel and reduced peak intensity.

The excellent match between individual scans in Fig. 3 shows the reproducibly of the technique. Furthermore, one can choose for how many cycles the delay value is kept. This allows, for example, dwelling at a certain delay step for a given number of shots to increase the signal-to-noise ratio by averaging.

Figure 4A shows the cross-correlation function recorded by generating sum frequency in a 1-mm-thick BBO crystal between the outputs of the 2 RAs in the case when, for each delay, 400 shots were accumulated. In Fig. 4B, the intensity distribution for 4 selected delay values corresponding to the steepest slope of the cross-correlation signal are plotted. Figure 4C shows the corresponding timing jitter as obtained by the slope of the signal from Fig. 4A. Most jitter originates from an uncertainty of the trigger signal, which is in the order of one step size ($\Delta t = 80$ fs). More details on the trigger uncertainty are supplied in the Supplementary Materials.

To demonstrate the versatility and flexibility of the presented technique, transient absorption measurements of a perovskite sample (polycrystalline thin film of $CH_3NH_3PbI_3$) were performed using a 2-color pump–probe setup, which is shown schematically in Fig. 5. Probe pulses with a bandwidth of 15 nm were generated in a non-collinear optical parametric amplifier (NOPA), tuned to 760 nm near the bandgap of the material. The pump pulses at 525 nm were obtained by frequency doubling the fundamental output of the other RA, providing more than 780 meV of excess energy above the bandgap. The pump fluence during the experiments was kept at less than 10% level with respect to the fluence at which features of permanent photo-bleaching of

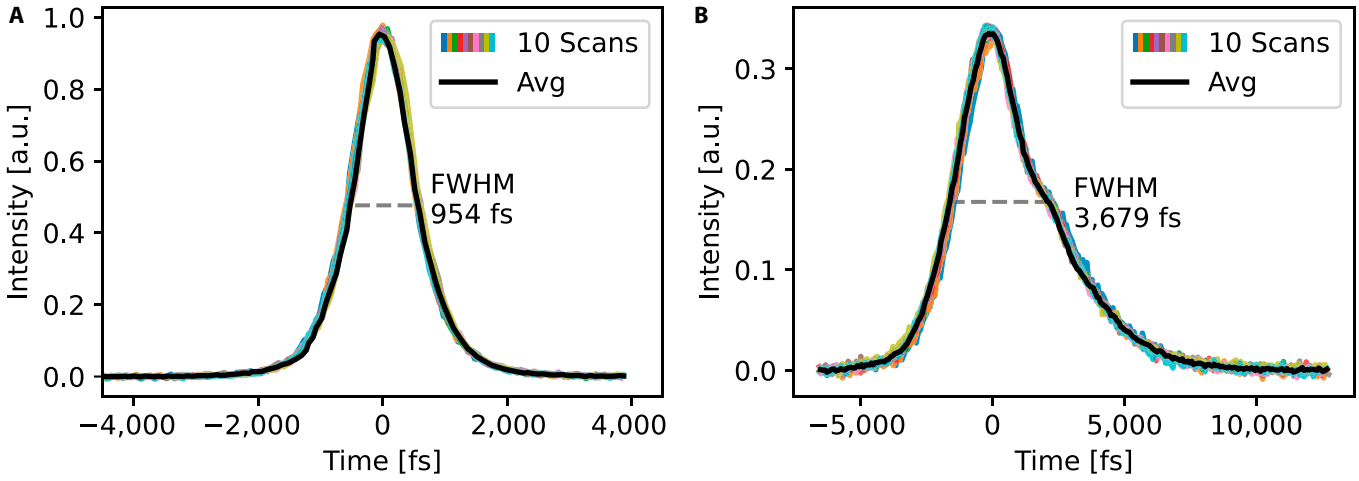

Fig. 3. (A) Direct cross-correlation measurements between the 2 output channels with ~80 fs step size. (B) Same as (A) with one of the compressor channels detuned.

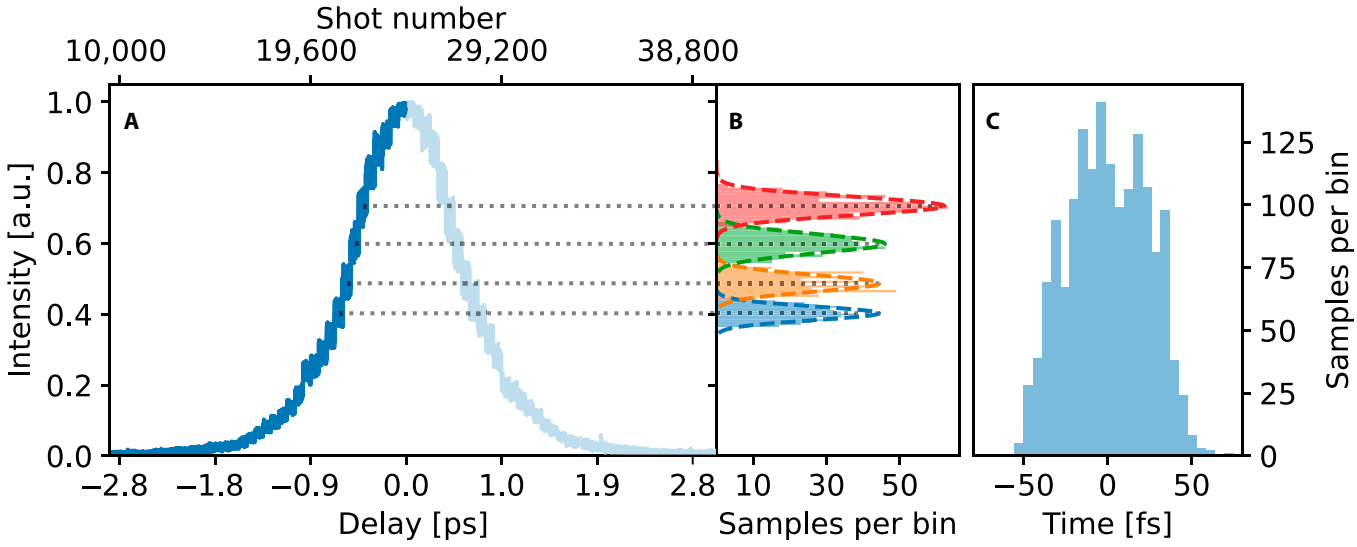

Fig. 4. (A) Measured cross-correlation with 400 points per delay. (B) Intensity distributions for 4 delay values. (C) Corresponding timing jitter distribution.

the sample was observed after irradiation for about 30 min. The initial time zero was found by placing a thin BBO nonlinear optical crystal at the sample position and generating sum frequency between the pump and probe pulses.

Figure 6 shows the dynamics of photoinduced transmission changes acquired for delays up to 50 ns with user controllable step sizes varying from 80 fs at early times to 512 ps at longer delays. The transient was recorded using a photodiode and a lock-in amplifier. A total of 463 data points were recorded in under 6 min. An electronic chopper was implemented by firing the RA for the pump pulses at half the repetition rate (250 Hz). The ultrafast photophysics of $CH_3NH_3PbI_3$ was studied in detail before [20]. The data in Fig. 6 represent the dynamics of the transmission at a probe wavelength of around 760 nm, where the photoinduced absorption due to bandgap renormalization [21], which leads to a red shift of the absorption band, dominates at short delay times. As charge carriers cool down and relay to the band edge, this photoinduced absorption is gradually transformed to the photobleaching characteristic of thermalized excitons and free carriers, causing a change in sign of the transmission changes. Formation of the positive signal takes place within 2 ps, in agreement with previous studies [20,21]. Afterwards, the signal decay on the nanosecond time scale reflects a mixture of trap-assisted recombination and Auger recombination, the dynamics of which are highly dependent on material preparation methods [21,22].

Conclusion

In conclusion, we have demonstrated a versatile scheme for the flexible generation of amplified femtosecond pulse pairs with rapidly variable, electronically tunable delays ranging from femtoseconds to milliseconds with femtosecond precision, enabled by a low-noise, spatially multiplexed, single-cavity, femtosecond, dual-comb solid-state oscillator in combination with a twin amplifier. In the demonstrated implementation, the timing uncertainty between 2 arbitrarily delayed amplifier pulses is limited to the delay step $\Delta t = \Delta f_{rep}/(f_{rep1,2})^2$, which, in our case, was 80 fs at $\Delta f_{rep} = 500$ Hz rate. However, by pairing such system with a single-cavity dual-comb oscillator at 1 GHz repetition rate [23], 1 fs timing uncertainty at 1 kHz amplifier rate can be achieved.

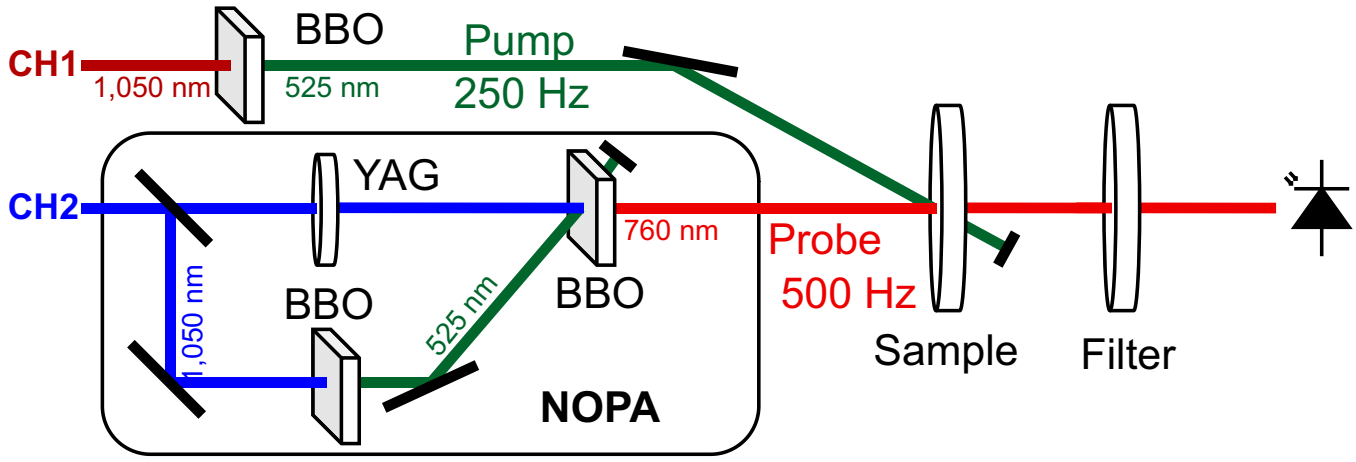

Fig. 5. Two-color pump–probe setup. One output channel is frequency doubled in a BBO crystal and used as a pump. The second output is frequency converted to 760 nm in a noncollinear optical parametric amplifier. YAG: undoped, for white light seed generation.

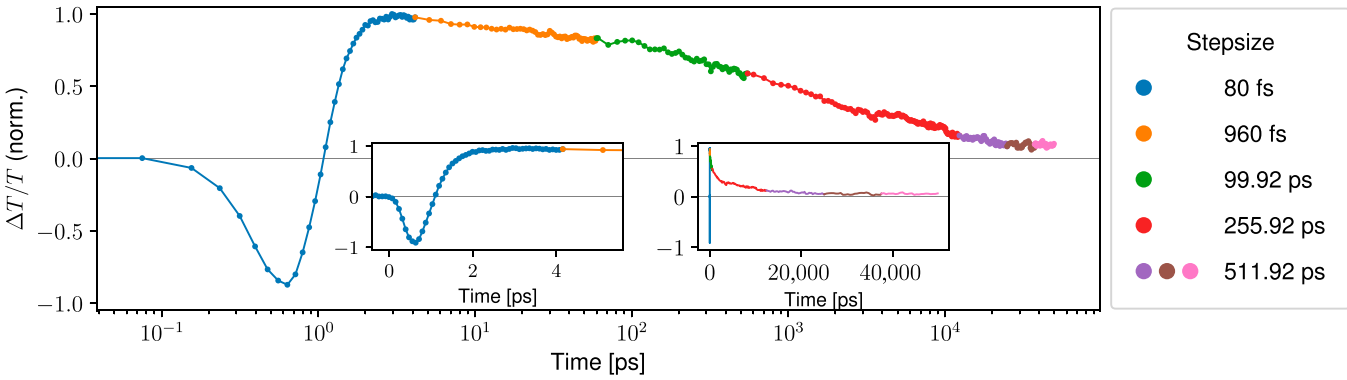

Fig. 6. Pump–probe data of the perovskite sample recorded over 50 ns with varying resolution and logarithmic time axis. The insets show the data with linear time axis in 2 different time scales. The legend denotes the step sizes used for each time scale. The color coding marks intervals in the range of the inverse repetition rate of the used oscillator ($1/f_{rep1,2} \cong 12.5$ ns) for which the pulse index offset (k) was kept constant.

The presented approach allows the recording of dynamics in nonlinear transient absorption spectroscopies ranging over orders of magnitude, from femtoseconds to milliseconds. We envisage that, besides the present use in ultrafast optical spectroscopy, the presented method will also enable several new applications in nonlinear beam steering and time/frequency to space mapping by utilizing presented rapid delay control for time-gating intense chirped pulses.

Acknowledgments

We acknowledge Patrice Camy (CIMAP) for providing the Yb:CaF_2 crystal used in the single-cavity dual-comb laser. **Funding:** This work was supported by FWF (4566) and Schweizerischer Nationalfonds zur Förderung der Wissenschaftlichen Forschung (40B1-0_203709 and 40B2-0_180933). **Competing interests:** The authors declare that they have no competing interests.

Data Availability

The data that support the plots within this article and other findings of the study are available from the corresponding authors upon reasonable request.

Supplementary Materials

Supplemental document: See Supplement 1 for supporting content.

References

1. Maiuri M, Garavelli M, Cerullo G. Ultrafast spectroscopy: State of the art and open challenges. *J Am Chem Soc*. 2020;142(1):3–15.
2. Bredenbeck J, Helbing J, Sieg A, Schrader T, Zinth W, Renner C, Behrendt R, Moroder L, Wachtveitl J, Hamm P. Picosecond conformational transition and equilibration of a cyclic peptide. *Proc Natl Acad Sci U S A*. 2003;100(11):6452–6457.
3. Guo Z, Wan Y, Yang M, Snaider J, Zhu K, Huang L. Long-range hot-carrier transport in hybrid perovskites visualized by ultrafast microscopy. *Science*. 2017;356(6333):59–62.
4. Weingarten KJ, Rodwell MJW, Heinrich HK, Kolner BH, Bloom DM. Direct electro-optic sampling of GaAs integrated circuits. *Electron Lett*. 1985;21(17):765–766.
5. Elzinga PA, Kneisler RJ, Lytle FE, Jiang Y, King GB, Laurendeau NM. Pump/probe method for fast analysis of visible spectral signatures utilizing asynchronous optical sampling. *Appl Opt*. 1987;26(19):4303–4309.

6. Picqué N, Hänsch TW. Frequency comb spectroscopy. *Nat Photonics*. 2019;13:146–157.
7. Coddington I, Newbury N, Swann W. Dual-comb spectroscopy. *Optica*. 2016;3(4):414–426.
8. de Boeij WP, Wiersma DA. Ultrafast solvation dynamics explored by nonlinear optical spectroscopy [thesis]. [Groningen]: University of Groningen; 1997.
9. Bredenbeck J, Helbing J, Hamm P. Continuous scanning from picoseconds to microseconds in time resolved linear and nonlinear spectroscopy. *Rev Sci Instrum*. 2004;75(11):4462–4466.
10. Jones DJ, Potma EO, Cheng J, Burfeindt B, Pang Y, Ye J, Xie XS. Synchronization of two passively mode-locked, picosecond lasers within 20 fs for coherent anti-stokes Raman scattering microscopy. *Rev Sci Instrum*. 2002;73(8):2843–2848.
11. Fourkas JT, Dhar L, Nelson KA, Trebino R. Spatially encoded, single-shot ultrafast spectroscopies. *J Opt Soc Am B*. 1995;12(1):155–165.
12. Greetham GM, Donaldson PM, Nation C, Sazanovich Iv, Clark IP, Shaw DJ, Parker AW, Towrie M. A 100 kHz time-resolved multiple-probe femtosecond to second infrared absorption spectrometer. *Appl Spectrosc*. 2016;70(4):645–653.
13. Antonucci L, Solinas X, Bonvalet A, Joffre M. Asynchronous optical sampling with arbitrary detuning between laser repetition rates. *Opt Express*. 2012;20(16):17928–17937.
14. Antonucci L, Bonvalet A, Solinas X, Daniault L, Joffre M. Arbitrary-detuning asynchronous optical sampling with amplified laser systems. *Opt Express*. 2015;23(21):27931–27940.
15. Solinas X, Antonucci L, Bonvalet A, Joffre M. Multiscale control and rapid scanning of time delays ranging from picosecond to millisecond. *Opt Express*. 2017;25(15):17811–17819.
16. Pupeikis J, Willenberg B, Camenzind SL, Benayad A, Camy P, Phillips CR, Keller U. Spatially multiplexed single-cavity dual-comb laser. *Optica*. 2022;9(7):713–716.
17. Shelton R, Ma L-S, Kapteyn H, Murnane M, Hall J, Ye J. Active synchronization and carrier phase locking of two separate mode-locked femtosecond lasers. *J Mod Opt*. 2002;49(3–4):401–409.
18. Gebs R, Klatt G, Janke C, Dekorsy T, Bartels A. High-speed asynchronous optical sampling with sub-50fs time resolution. *Opt Express*. 2010;18(6):5974–5983.
19. Camenzind SL, Koenen D, Willenberg B, Pupeikis J, Phillips CR, Keller U. Timing jitter characterization of free-running dual-comb laser with sub-attosecond resolution using optical heterodyne detection. *Opt Express*. 2022;30(4):5075–5094.
20. Richter JM, Branchi F, Valduga de Almeida Camargo F, Zhao B, Friend RH, Cerullo G, Deschler F. Ultrafast carrier thermalization in lead iodide perovskite probed with two-dimensional electronic spectroscopy. *Nat Commun*. 2017;8:Article 376.
21. Ghosh T, Aharon S, Etgar L, Ruhman S. Free carrier emergence and onset of electron–phonon coupling in methylammonium lead halide perovskite films. *J Am Chem Soc*. 2017;139(50):18262–18270.
22. Pazos-Outón LM, Xiao TP, Yablonovitch E. Fundamental efficiency limit of lead iodide perovskite solar cells. *J Phys Chem Lett*. 2018;9(7):1703–1711. https://doi.org/10.1021/acs.jpclett.7b03054
23. Phillips CR, Willenberg B, Nussbaum-Lapping A, Callegari F, Camenzind SL, Pupeikis J, Keller U. Coherently averaged dual-comb spectroscopy with a low-noise and high-power free-running gigahertz dual-comb laser. *Optics Express*. 2023;31(5):7103.